Dynamic modelling of an Isoglide T3 type parallel robot

Nadia Cretescu[1] and Mircea Neagoe[1]

[1] Renewable Energy Systems and Recycling R&D Center, Transilvania University of Brasov, Romania

ncretescu@unitbv.ro, mneagoe@unitbv.ro

Abstract. The dynamic modelling of parallel robots rise difficult development issues due to the structural, kinematic and dynamic complexity of parallel mechanisms. The paper presents the application of a dynamic approach aiming at reducing the modelling complexity by replacing the parallel robotic structure with simpler open kinematic chains derived from the parallel structure. This method was successfully applied to obtain the closed-form dynamic model of an Isoglide T3 parallel robot and it was validated by numerical simulations using the ADAMS software.

Keywords: Parallel robots, dynamic modelling, closed-form dynamic model, simulation, ADAMS software.

1 Introduction

The parallel robots are closed kinematic chain type mechanisms, composed by a mobile platform connected to the base by two or more kinematic arms (legs or limbs). For each arm a simple open or a complex kinematic chain can be associated [1].

The parallel robots have the advantages of higher speeds and precision, higher loads and stiffness comparing with serial manipulators. The most important drawback is related their reduced workspace.

Different approaches can be applied to obtain the dynamic model of parallel robots, e.g. Euler-Lagrange method, Lagrange equations with multipliers, Newton-Euler method, were applied in literature aiming at identifying their dynamic behaviour [2-7]. A dynamic modelling method for hybrid robotic structures is presented in [8]. The direct and inverse dynamic models of the robotic arms and the mobile platform were obtained by using the Newton Euler equations, where Jacobian matrices are also involved.

The influence of the load-rigidity correlation on the dynamic response of a medical Triglide parallel robot was identified using ADAMS simulations in the hypothesis of rigid and elastic connecting rods [9]. The same approach was applied for a 4 DOF parallel robot of type T3R1with decoupled motions [10]. The Lagrange with multipliers method was used in [11] to obtain the analytical dynamic models of two parallel robots with two and three degrees of coupling, respectively, followed by a virtual simulation in SimMechanics environment.

The Lagrange equations of second kind is used in this paper to derive the closed-form dynamic model of an Isoglide T3 parallel robot, considering the rigid link hypothesis, based on an approach presented by Ibrahim [12]. The structural and kinematic analysis is presented in Section 3, followed by the analytical dynamic modelling of the three open arms and the end-effector platform and the projection of the dynamic equations in the space of active joints (Section 4), developed using the Maple software. The close-form dynamic model is numerically simulated and validated in the ADAMS environment software (Section 5). The conclusions of the study are drawn in the section 6.

2 Problem formulation

The dynamic modelling of parallel type robotic structures, used in this paper, is based on an algorithm proposed by Ibrahim [12] and composed of the following steps:
1) breaking the kinematic joints between the mobile platform (end-effector) and the component robotic arms;
2) inverse dynamic modelling of each open robotic arm with serial kinematic chain configuration, considering the joint variables as independent generalized coordinates;
3) inverse dynamic modelling of the end-effector platform based on the operational variables associated to the parallel robot, considering known the end-effector motion;
4) projection of the dynamic equations obtained for the open robotic arms and the mobile platform into the space of the independent joint variables (in the active joints) of the parallel robot through Jacobian matrices.
The dynamic modelling of the robot arms, considered after removing their connections with the end-effector platform, can be done using known approaches applied to serial robots, such as the Newton-Euler method or Lagrange equations of the second kind. The inverse dynamic model of the end-effector platform can be described through the Newton-Euler equations, which allow to obtain the forces and moments applied on a rigid body with known motion.
The inverse dynamic modelling algorithm of each robotic arm, isolated from the parallel robot, has the following steps:

- establishing the kinetic energy of the component kinematic links;
- establishing the potential energy of the component kinematic links;
- expressing the Lagrangian of the robotic arm;
- deriving the inverse dynamic equations for each arm.

The generalized forces (forces and torques) resulting in the inverse dynamic models of the end-effector platform and the robotic arms, considered independently, are reduced in the space of active joints and thus the actuating generalized forces are obtained by applying the superposition principle.

3 Geometric and Kinematic Modelling

The Isoglide T3 robot has a three degrees of freedom (DOF) parallel structure of 3TRRR type (3 **T**ranslation, **R**otation, **R**otation, **R**otation) with three translational inputs and three translational outputs (Fig.1). It is composed by a mobile end-effector platform (4) connected to the base by three arms *a, b c*, each one composed by three links (1_i, 2_i, 3_i, where $i = a, b, c$) and four kinematic joints: one active prismatic joint disposed along the axis of the global coordinate system $O_0X_0Y_0Z_0$ (denoted by q_i, $i = a, b, c$) and 3 passive revolute joints characterized by the relative angular displacements φ_{1i}, φ_{2i}, φ_{3i}, where $i = a, b, c$. The four joints have parallel axes to each other.

The three output motions of the end-effector along the axes X_0, Y_0 and Z_0 are decoupled. Therefore, each output motion is commanded from a single motor: the output motion along the X_0 axis is controlled by the active joint q_a, the one along the Y_0 axis by the active joint q_b, and the one along Z_0 axis by the active joint q_c. In addition, the input motions are transmitted unchanged to the outputs [13]. Therefore, this parallel robot type is also called "maximally regular" [14, 15] and refers to the particular case of Jacobian matrix that equals the identity matrix.

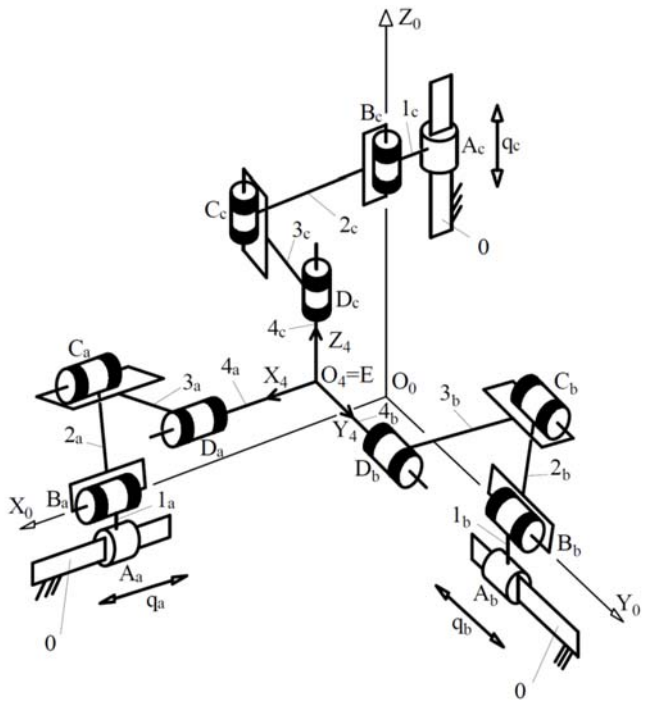

Fig. 1. Kinematic diagram of an Isoglide T3 parallel robot

The traveling coordinate system method [16] was used to obtain the direct and inverse geometric and kinematic models of the Isoglide T3 parallel robot. The results of the direct geometric model is the absolute translational displacement function, i.e. the displacements of the end-effector characteristic point $E(x_E, y_E, z_E) \equiv O_4$ in relation with the relative displacements in the active joints (q_a, q_b, q_c):

$$\begin{cases} x_E = q_a - l_{4a} \\ y_E = q_b - l_{4b} \\ z_E = q_c - l_{4c} \end{cases} \tag{1}$$

where l_{4a}, l_{4b}, l_{4c} represent the lengths of the mobile platform 4 in the direction of the axes of the local coordinate system $O_4X_4Y_4Z_4$ as depicted in Fig. 1.

The inverse geometric model allows to establish the dependence of the relative displacements in the active joints (q_a, q_b, q_c), in relation with the end-effector Cartesian coordinates (x_E, y_E, z_E):

$$\begin{cases} q_a = x_E + l_{4a} \\ q_b = y_E + l_{4b} \\ q_c = z_E + l_{4c} \end{cases} \tag{2}$$

The direct kinematic model expresses the dependences of the end-effector speeds ($\dot{x}_E$, $\dot{y}_E$, $\dot{z}_E$) and acceleration ($\ddot{x}_E$, $\ddot{y}_E$, $\ddot{z}_E$) on the relative linear speeds ($\dot{q}_a$, $\dot{q}_b$, $\dot{q}_c$) and accelerations ($\ddot{q}_a$, $\ddot{q}_b$, $\ddot{q}_c$) in the active joints, through the robot Jacobian matrix J_e:

$$\begin{bmatrix} \dot{x}_E \\ \dot{y}_E \\ \dot{z}_E \end{bmatrix} = J_e \cdot \begin{bmatrix} \dot{q}_a \\ \dot{q}_b \\ \dot{q}_c \end{bmatrix} \quad \text{and} \quad \begin{bmatrix} \ddot{x}_E \\ \ddot{y}_E \\ \ddot{z}_E \end{bmatrix} = \dot{J}_e \cdot \begin{bmatrix} \dot{q}_a \\ \dot{q}_b \\ \dot{q}_c \end{bmatrix} + J_e \cdot \begin{bmatrix} \ddot{q}_a \\ \ddot{q}_b \\ \ddot{q}_c \end{bmatrix} \tag{3}$$

where J_e and $\dot{J}_e$ are define by relations:

$$J_e = \begin{bmatrix} \frac{\partial x_E}{\partial q_a} & \frac{\partial x_E}{\partial q_b} & \frac{\partial x_E}{\partial q_c} \\ \frac{\partial y_E}{\partial q_a} & \frac{\partial y_E}{\partial q_b} & \frac{\partial y_E}{\partial q_c} \\ \frac{\partial z_E}{\partial q_a} & \frac{\partial z_E}{\partial q_b} & \frac{\partial z_E}{\partial q_c} \end{bmatrix} = \begin{bmatrix} 1 & 0 & 0 \\ 0 & 1 & 0 \\ 0 & 0 & 1 \end{bmatrix} \quad \text{and } \dot{J}_e = \begin{bmatrix} 0 & 0 & 0 \\ 0 & 0 & 0 \\ 0 & 0 & 0 \end{bmatrix}. \tag{4}$$

As a result, the kinematical model is expressed by:

$$\begin{bmatrix} \dot{x}_E \\ \dot{y}_E \\ \dot{z}_E \end{bmatrix} = \begin{bmatrix} \dot{q}_a \\ \dot{q}_b \\ \dot{q}_c \end{bmatrix} \quad \text{and} \quad \begin{bmatrix} \ddot{x}_E \\ \ddot{y}_E \\ \ddot{z}_E \end{bmatrix} = \begin{bmatrix} \ddot{q}_a \\ \ddot{q}_b \\ \ddot{q}_c \end{bmatrix}. \tag{5}$$

4 Dynamic modelling

The inverse dynamic modelling begins for the Isoglide T3 parallel robot with the preliminary stage of disconnecting the three arms from the mobile platform, i.e. disassembling the passive revolute joints D_a, D_b and D_c as represented in Fig. 2. Thus, three separate kinematic open chains of T-R-R type (the arms 1_j-2_j-3_j, $j = a, b, c$) and the end-effector 4 are obtained.

The three robotic arms a, b and c have a serial structure, formed by the active prismatic joints A_j and two passive revolute joints B_j and C_j, $j = a, b, c$, Fig. 2. The three kinematic joints A_j, B_j and C_j have axes parallel to the axis O_0x_0 for the robotic arm a, with axis O_0y_0 for the robotic arm b and to the axis O_0z_0 for the robotic arm c, respectively. The independent joint variables (the linear relative displacement in the active joints A_j) are denoted by q_j, and the dependent ones by φ_{1j} for the joints B_j and by φ_{2j} for the joints C_j, $j = a, b, c$.

The links of the robotic arms are rigid bodies and characterized by the length l_k (distance between the axes of the two adjacent joints), the gravity centre G_k, the mass m_k and the matrix of the moments of inertia J_k established in a local coordinate system with origin point in the gravity centre G_k, $k = 1_a, 2_a, 3_a, 1_b, 2_b, 3_b, 1_c, 2_c, 3_c$. As a simplifying hypothesis, the gravity centres G_k are located at middle of the length l_k and the centrifugal moments of inertia are zero (i.e. the axes of the local coordinate system coincide with the axes of inertia of the link).

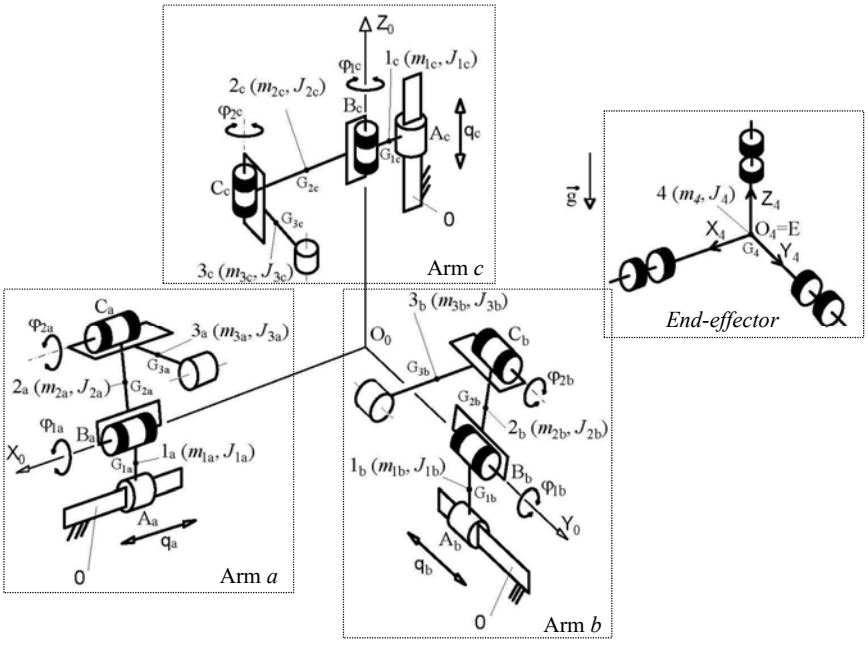

Fig. 2. Dynamic scheme of the Isoglide T3 robot considering the robotic arms detached from the end-effector platform.

The end-effector platform 4 performs only translational motions, it has the mass m_4 and the gravity centre G_4 in the origin O_4 of the local coordinate system $O_4X_4Y_4Z_4$, as well as the matrix of moments of inertia J_4. The length of the element 4 in the X_4 direction is denoted by l_{4a}, in the Y_4 direction by l_{4b} and in the Z_4 direction by l_{4c}.

The inverse dynamic model of the Isoglide T3 parallel robot is derived based on the following algorithm:

1. Stage I: inverse dynamic modelling of the 3 robotic arms *a*, *b* and *c*, considered as independent serial kinematic chains. The Lagrange equations of second kind are used in this study.
2. Stage II: inverse dynamic modelling of the end-effector platform 4, considered as a rigid body with independent translational motions along the three axes of the global coordinate system $O_0X_0Y_0Z_0$.
3. Stage III: projection of the dynamic equations of the robotic arms and of the end-effector platform in the force space of the active joints A_j, $j = a, b, c$, Fig. 2.

4.1 Inverse dynamic models of the robotic arms

The inverse dynamic modelling based on the Lagrange equations of second kind, in the case of a robotic arm $j = a, b, c,$ involves determining the total kinetic energy K_j and the total potential energy P_j, necessary to establish the system Lagrangian L_j:

$$L_j = K_j - P_j = \sum_{i=1}^{3} K_{ij} - \sum_{i=1}^{3} P_{ij} \,, \tag{6}$$

where K_{ij} represent the kinematical energy of the i^{th} link from the arm j:

$$K_{ij} = \frac{1}{2} m_{ij} v_{Gij}^2 + \frac{1}{2} \omega_{ij}^T J_{Gij} \omega_{ij} \,,\; J_{Gij} = \begin{bmatrix} J_{ijxx} & 0 & 0 \\ 0 & J_{ijyy} & 0 \\ 0 & 0 & J_{ijzz} \end{bmatrix}, \tag{7}$$

where m_{ij} is the mass of the link ij, v_{Gij} – the speed of the gravity centre G_{ij}, ω_{ij} – the angular speed vector of the link ij, J_{Gij} – the inertial matrix of the link ij, define in a local coordinate system $O_{ij}x_{ij}y_{ij}z_{ij}$ with the origin O_{ij} in the gravity centre G_{ij} and with the axes parallel to the principal axis of inertia, J_{ijxx}, J_{ijyy}, J_{ijzz} – principal moments of inertia in relation with the axis x_{ij}, y_{ij} and z_{ij}.

The potential energy P_{ij} of the link ij is determined by using:

$$P_{ij} = -m_{ij} \vec{g} \cdot \vec{r}_{Gij} = m_{ij} g \cdot z_{Gij} \,, \tag{8}$$

where $\vec{r}_{Gij} = x_{Gij}\vec{i}_0 + y_{Gij}\vec{j}_0 + z_{Gij}\vec{k}_0$ is the position vector of the gravity centre G_{ij} in global coordinate system, $\vec{i}_0, \vec{j}_0, \vec{k}_0$ – the unit vectors of the global coordinate system axes, $\vec{g} = -g\vec{k}_0$ is the gravitational acceleration, Fig. 2.

Using the geometric and kinematic models, the Langrangian L_j of the robotic arm j is described by:

$$L_j = \frac{1}{2} A_{0j} \ddot{q}_j^2 + \frac{1}{2} A_{1j} \dot{\varphi}_{1j}^2 + \frac{1}{2} A_{2j} \dot{\varphi}_{2j}^2 + A_{3j} \dot{\varphi}_{1j} \dot{\varphi}_{2j} + A_{4j} g \ , \ j = a, b, c \tag{9}$$

where

$$\begin{cases} A_{0j} = m_{1j} + m_{2j} + m_{3j} \\ A_{1j} = J_{2j} + J_{3j} + m_{2j} c_{2j}^2 + m_{3j} \left(l_{2j}^2 + c_{3j}^2 \right) + 2 m_{3j} l_{2j} c_{3j} \cos \varphi_{2j} \\ A_{2j} = J_{3j} + m_{3j} c_{3j}^2 \\ A_{3j} = J_{3j} + m_{3j} c_{3j}^2 + m_{3j} l_{2j} c_{3j} \cos \varphi_{2j} \\ A_{4a} = m_{1a} c_{1a} - m_{2a} c_{2a} \sin \varphi_{1a} - m_{3a} l_{2a} \sin \varphi_{1a} - m_{3a} c_{3a} \sin \left(\varphi_{1a} + \varphi_{2a} \right) \\ A_{4b} = m_{1b} c_{1b} - m_{2b} c_{2b} \cos \varphi_{1b} - m_{3b} l_{2b} \cos \varphi_{1a} - m_{3b} c_{3b} \cos \left(\varphi_{1b} + \varphi_{2b} \right) \\ A_{4c} = -\left(m_{1c} + m_{2c} + m_{3c} \right) q_c \end{cases} \tag{10}$$

with notation $J_{2a} = J_{2axx}$, $J_{3a} = J_{3axx}$, $J_{2b} = J_{2byy}$, $J_{3b} = J_{3byy}$, $J_{2c} = J_{2czz}$, $J_{3c} = J_{3czz}$, and $c_{1j} = B_j G_{1j}$, $c_{2j} = B_j G_{2j}$ and $c_{3j} = C_j G_{3j}$ (Fig. 2).

After performing the calculus according to Lagrange equations, the inverse dynamic model of a robotic arm j is expressed by:

$$\begin{bmatrix} F_j \\ \tau_{1j} \\ \tau_{2j} \end{bmatrix} = M_j \cdot \begin{bmatrix} \ddot{q}_j \\ \ddot{\varphi}_{1j} \\ \ddot{\varphi}_{2j} \end{bmatrix} + V_j \begin{bmatrix} \dot{q}_j \\ \dot{\varphi}_{1j} \\ \dot{\varphi}_{2j} \end{bmatrix} + G_j \ , j = a, b, c \tag{11}$$

where: Fj-, τ_{ij}-, Mj represents the matrix of inertial coefficients, Vj - the matrix of centrifugal and Coriolis coefficients, and Gj - the vector of gravitational terms:

$$M_j = \begin{bmatrix} A_{0j} & 0 & 0 \\ 0 & A_{1j} & A_{3j} \\ 0 & A_{3j} & A_{2j} \end{bmatrix} \tag{12}$$

$$V_j = \begin{bmatrix} 0 & 0 & 0 \\ 0 & -2 m_{3j} l_{2j} c_{3j} \sin \varphi_{2j} \dot{\varphi}_{2j} & -m_{3j} l_{2j} c_{3j} \sin \varphi_{2j} \dot{\varphi}_{2j} \\ 0 & m_{3j} l_{2j} c_{3j} \sin \varphi_{2j} \dot{\varphi}_{1j} & 0 \end{bmatrix} \tag{13}$$

$$G_a = \begin{bmatrix} 0 \\ m_{2a} c_{2a} \cos \varphi_{1a} + m_{3a} (l_{2a} \cos \varphi_{1a} + c_{3a} \cos(\varphi_{1a} + \varphi_{2a})) \\ m_{3a} c_{3a} \cos(\varphi_{1a} + \varphi_{2a}) \end{bmatrix} \tag{14a}$$

$$G_b = \begin{bmatrix} 0 \\ -m_{2b}c_{2b}\sin\varphi_{1b} - m_{3b}(l_{2b}\sin\varphi_{1b} + c_{3b}\sin(\varphi_{1b}+\varphi_{2b})) \\ -m_{3b}c_{3b}\sin(\varphi_{1b}+\varphi_{2b}) \end{bmatrix} \tag{14b}$$

$$G_c = \begin{bmatrix} m_{1c}+m_{2c}+m_{3c} \\ 0 \\ 0 \end{bmatrix} \tag{14a}$$

4.2 Inverse dynamic model of the end-effector platform

As the mobile platform can only perform translational motions, and considering the Eq. (5), the inverse dynamic model is expressed by:

$$F_4 = \begin{bmatrix} F_{4x} \\ F_{4y} \\ F_{4z} \end{bmatrix} = \begin{bmatrix} m_4\ddot{q}_a \\ m_4\ddot{q}_b \\ m_4(\ddot{q}_c - g) \end{bmatrix}. \tag{15}$$

4.3 Projection of the dynamic equations in the force space of the active joints

The dynamic model of a robotic arm j can be projected in the force space of the active joints by applying the principle of virtual power:

$$\begin{bmatrix} F_j \\ \tau_{1j} \\ \tau_{2j} \end{bmatrix}^T \cdot \begin{bmatrix} \dot{q}_j \\ \dot{\varphi}_{1j} \\ \dot{\varphi}_{2j} \end{bmatrix} = \begin{bmatrix} F_{a.j} \\ F_{b.j} \\ F_{c.j} \end{bmatrix}^T \cdot \begin{bmatrix} \dot{q}_a \\ \dot{q}_b \\ \dot{q}_c \end{bmatrix}, j = a, b, c \tag{16}$$

where $F_{a.j}$, $F_{b.j}$ and $F_{c.j}$ represent the components of the forces in the active joints generated by the dynamic effects of the robotic arm j.
It is known that:

$$\begin{bmatrix} \dot{q}_j \\ \dot{\varphi}_{1j} \\ \dot{\varphi}_{2j} \end{bmatrix} = J_{qj} \cdot \begin{bmatrix} \dot{q}_a \\ \dot{q}_b \\ \dot{q}_c \end{bmatrix} \rightarrow \begin{bmatrix} F_{a.j} \\ F_{b.j} \\ F_{c.j} \end{bmatrix} = J_{qj}^T \begin{bmatrix} F_j \\ \tau_{1j} \\ \tau_{2j} \end{bmatrix} \tag{17}$$

where

$$J_{qj} = \begin{bmatrix} \dfrac{\partial q_j}{\partial q_a} & \dfrac{\partial q_j}{\partial q_b} & \dfrac{\partial q_j}{\partial q_c} \\ \dfrac{\partial \varphi_{1j}}{\partial q_a} & \dfrac{\partial \varphi_{1j}}{\partial q_b} & \dfrac{\partial \varphi_{1j}}{\partial q_c} \\ \dfrac{\partial \varphi_{2j}}{\partial q_a} & \dfrac{\partial \varphi_{2j}}{\partial q_b} & \dfrac{\partial \varphi_{2j}}{\partial q_c} \end{bmatrix}. \tag{18}$$

The absolute positions of the central points of the passive joint D_j, $j = a, b, c$ can be expressed depending on both the operational variables (x_E, y_E, z_E) and on the joint variables (q_j, φ_{1j}, φ_{2j}). The relationships thus obtained make possible to obtain the partial derivatives in the matrix (18):

$$J_{qa} = \begin{bmatrix} 1 & 0 & 0 \\ 0 & \dfrac{\cos(\varphi_{1a} + \varphi_{2a})}{l_{2a} \sin \varphi_{2a}} & \dfrac{\sin(\varphi_{1a} + \varphi_{2a})}{l_{2a} \sin \varphi_{2a}} \\ 0 & \dfrac{-l_{2a} \cos \varphi_{1a} - l_{3a} \cos(\varphi_{1a} + \varphi_{2a})}{l_{2a} l_{3a} \sin \varphi_{2a}} & \dfrac{-l_{2a} \sin \varphi_{1a} - l_{3a} \sin(\varphi_{1a} + \varphi_{2a})}{l_{2a} l_{3a} \sin \varphi_{2a}} \end{bmatrix} \tag{19a}$$

$$J_{qb} = \begin{bmatrix} 1 & 0 & 0 \\ 0 & \dfrac{\sin(\varphi_{1b} + \varphi_{2b})}{l_{2b} \sin \varphi_{2b}} & \dfrac{\cos(\varphi_{1b} + \varphi_{2b})}{l_{2b} \sin \varphi_{2b}} \\ 0 & \dfrac{-l_{2b} \sin \varphi_{1b} - l_{3b} \sin(\varphi_{1b} + \varphi_{2b})}{l_{2b} l_{3b} \sin \varphi_{2b}} & \dfrac{-l_{2b} \cos \varphi_{1b} - l_{3b} \cos(\varphi_{1b} + \varphi_{2b})}{l_{2b} l_{3b} \sin \varphi_{2b}} \end{bmatrix} \tag{19b}$$

$$J_{qc} = \begin{bmatrix} 1 & 0 & 0 \\ 0 & \dfrac{\cos(\varphi_{1c} + \varphi_{2c})}{l_{2c} \sin \varphi_{2c}} & \dfrac{\sin(\varphi_{1c} + \varphi_{2c})}{l_{2c} \sin \varphi_{2c}} \\ 0 & \dfrac{-l_{2c} \cos \varphi_{1c} - l_{3c} \cos(\varphi_{1c} + \varphi_{2c})}{l_{2c} l_{3c} \sin \varphi_{2c}} & \dfrac{-l_{2c} \sin \varphi_{1c} - l_{3c} \sin(\varphi_{1c} + \varphi_{2c})}{l_{2c} l_{3c} \sin \varphi_{2c}} \end{bmatrix} \tag{19c}$$

Similarly, the dynamic equations of the end-effector platform are projected into the force space of the active joints using:

$$\begin{bmatrix} F_{a.4} \\ F_{b.4} \\ F_{c.4} \end{bmatrix} = J_e^T \begin{bmatrix} F_{4x} \\ F_{4y} \\ F_{4z} \end{bmatrix} \tag{20}$$

where J_e is the identity matrix according to Eq. (4).

By applying the superposition principle for the projected dynamic equations, the total driving forces in the active joints A_j, $j = a, b, c$ are:

$$\begin{bmatrix} F_{A_a} \\ F_{A_b} \\ F_{A_c} \end{bmatrix} = \begin{bmatrix} F_{a.a} \\ F_{b.a} \\ F_{c.a} \end{bmatrix} + \begin{bmatrix} F_{a.b} \\ F_{b.b} \\ F_{c.b} \end{bmatrix} + \begin{bmatrix} F_{a.c} \\ F_{b.c} \\ F_{c.c} \end{bmatrix} + \begin{bmatrix} F_{a.4} \\ F_{b.4} \\ F_{c.4} \end{bmatrix}. \tag{21}$$

5 Simulation results

The closed-form dynamic model described by Eq. (21), obtained by using the Maple software, was simulated on a test trajectory implemented both on Maple and ADAMS software, that allows the modelling and simulation of mechanisms as multibody systems (MBS) [17]. The CAD model of the Isoglide T3 parallel robot (Fig. 3) includes bodies of simple cylindrical shape; this ADAMS model can be used for validation of the closed-form model and to deliver the necessary input data in numerical simulations related to the inertial link properties, Table 1.

Table1. Geometric and inertial properties of the robot links

Link/ body	Length [m]	Mass [kg]	Principal moments of inertia [kg·m2]		
			Jxx	Jyy	Jzz
1*j*	0.1	0.98	$9.14 \cdot 10^{-4}$	$9.14 \cdot 10^{-4}$	$1.96 \cdot 10^{-4}$
2*j*	0.63	6.17	0.204	1.235·10-3	0.204
3*j*	0.63	6.17	0.204	1.235·10-3	0.204
4	0.20	5.66	$5.302 \cdot 10^{-2}$	$5.302 \cdot 10^{-2}$	$5.302 \cdot 10^{-2}$
$j = a, b, c$					

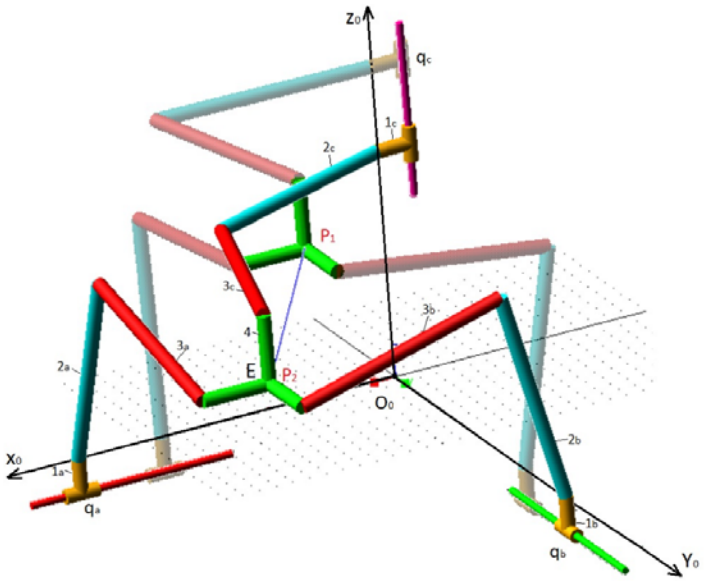

Fig. 3. ADAMS model of the Isoglide T3 parallel robot and its positions at the trajectory ends

The numerical simulations were performed on a trajectory defined in the joint space, characterized by:

- motion duration t = 10 s;
- strokes in active joints $\Delta q_a = \Delta q_b = 0.25$ m and $\Delta q_c = -0.25$;
- linear trajectory between the points $P_1(0.7, 0.8, 0.9)$ and $P_2(0.95, 1.05, 0.65)$;
- time interpolation functions: fifth degree polynomials, as represented in Fig. 4 for the active prismatic joint A_a.

The simulations on the selected test trajectory (Fig. 3) allowed obtaining the driving forces as depicted in Fig. 5…7.

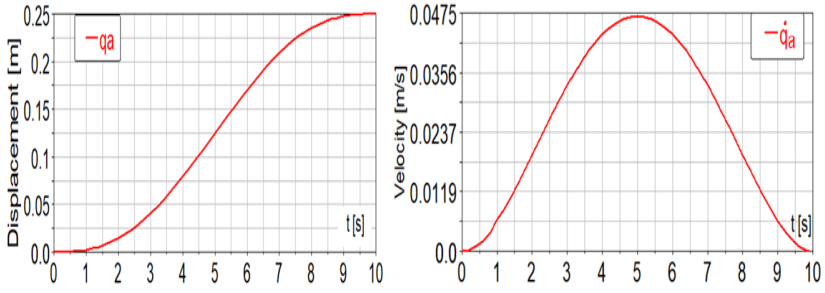

a b

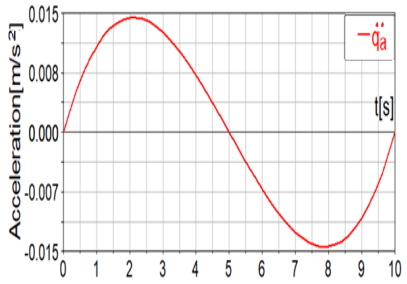

c

Fig. 4. Simulated motion for the active joint A_a: linear displacement q_a (a); linear speed $\dot{q}_a$ (b); linear acceleration $\ddot{q}_a$ (c).

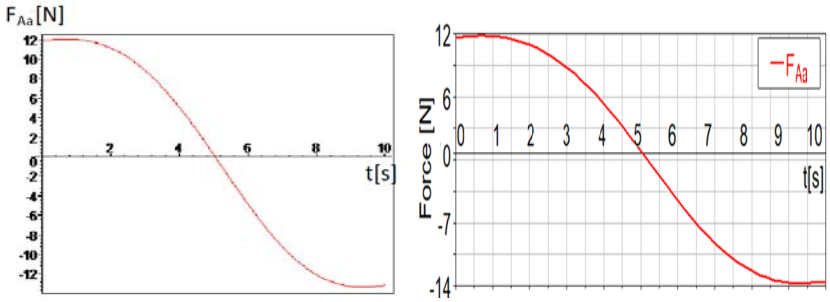

Fig. 5. Driving force F_{Aa} obtained by: numerical simulation in Maple (a); ADAMS simulation (b).

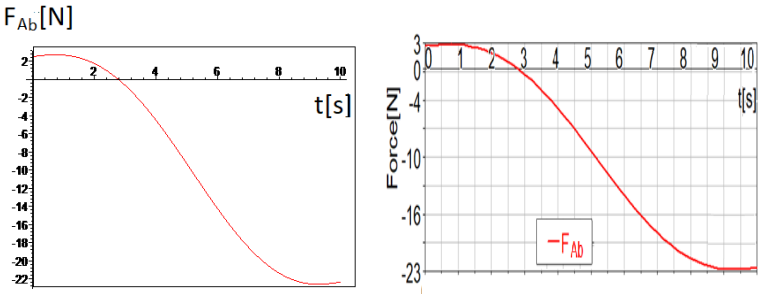

Fig. 6. Driving force F_{Ab} obtained by: numerical simulation in Maple (a); ADAMS simulation (b).

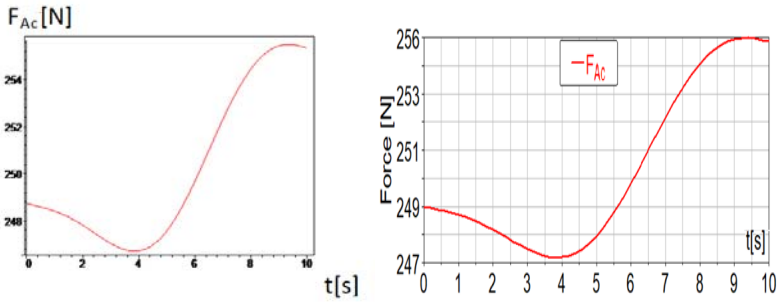

Fig. 7. Driving force F_{Ac} obtained by: numerical simulation in Maple (a); ADAMS simulation (b).

The analysis of the results obtained by numerical simulation of the closed-form model (Maple) and of the CAD model (ADAMS), it can be noticed that the driving forces have identical time variations for the same active joint in both cases (Figs. 5… 7). Thus, it can be concluded that the closed-form inverse dynamic model is validated by ADAMS simulation. It can also be observed that:

- the driving forces F_{Aa} and F_{Ab} follow the shape as the displacements imposed in the active joints (Fig. 5 and 6); the maximum values of the driving forces are ~12 N for the F_{Aa} force and ~22 N for the F_{Ab} force, respectively;
- the force F_{Ac} has higher values in relation to the other two driving forces (ranges between ~ 249 N up to ~ 255 N), due to the gravitational forces directed in the negative direction of the O_0z_0 axis.

6 Conclusion

The paper presents the inverse dynamic modelling of an Isoglide T3 parallel robot, using the approach of preliminary decomposing the parallel structure into open kinematic chains by disassembling the revolute joints between the robotic arms and the end-effector platform.

The application of the investigated inverse dynamic modelling for the Isoglide T3 parallel robot allowed to highlight the following aspects:

- By dismantling the revolute joints with the mobile platform, the parallel structure was decomposed into three serial robotic arms of TRR type and the end-effector link with translational motion;
- The inverse dynamic models of the three robotic arms, considered as independent mechanisms, were derived using the Lagrange equations of the second kind. The dynamic model of the mobile platform resulted based on the Newton's second law of motion;
- The driving forces were obtained by projecting the dynamic equations of the robotic arms and end-effector platform on the force space of the active joints, based on Jacobian matrices determined in the kinematic analysis stage;

- The closed-form of the inverse dynamic model was developed using the Maple software, that also allowed numerical simulation;
- The inverse dynamic model was validated by developing the CAD model of Isoglide T3 parallel robot and by simulating its dynamic behaviour using the ADAMS software.

The main advantages of the applied dynamic modelling method refer to the simplicity of its application: the complex modelling of a parallel structure is reduced to simpler modelling of serial structures (the robotic arms) and the end-effector platform, followed by the projection of their dynamic equations in the force space of the active joint through Jacobian matrices.

References

1. Gogu G., Structural synthesis of parallel robots. Part 1: Methodology, Springer Verlag, (2008).
2. Lee, K.M. , Shah, D.K. , Dynamic analysis of a three-degrees-of-freedom in-parallel actuated manipulator, IEEE Journal of Robotics and Automation, 4, pp. 361-368, (1988).
3. Bhattacharya, S., Nenchev, D.N., Uchiyama, M., A recursive formula for the inverse of the inertia matrix of a parallel manipulator, Mechanism and Machine Theory, 33 (7), pp. 957-964, (1998).
4. Liu, M-J., Li, C-X., Li, C-N., Dynamics analysis of the Gough–Stewart platform manipulator, IEEE Transaction on Robotics and Automation, 16 (1), pp. 94-98, (2000).
5. Dasgupta, B, Mruthyunjaya, T.S., A Newton–Euler formulation for the inverse dynamics of the Stewart platform manipulator, Mechanism and Machine Theory, 33 (8), pp. 1135-1152, (1998).
6. Dasgupta, B., Choudhury, P. , A general strategy based on the Newton–Euler approach for the dynamic formulation of parallel manipulators, Mechanism and Machine Theory, 34 (6), pp. 801-824, (1999).
7. Khalil, W., Guegan, S., Inverse and direct dynamic modeling of Gough–Stewart robots, IEEE Transactions on Robotics and Automation, 20 (4), pp. 754-762, (2004).
8. Ibrahim, O., Khalil, W., Inverse and direct dynamic models of hybrid robots, Mechanism and Machine Theory, pp 627-640, Vol 45, (2010).
9. Rat, N.R, Neagoe, M., Diaconescu, D., Stan, S.D. Dynamic simulations regarding the influence of the load-rigidity correlation on the working accuracy of a medical Triglide parallel robot, ISSN 1392 – 1207, MECHANIKA 17(2), pp 178-181, (2011).
10. Rat, N., Rizk, R., Gogu, G., Neagoe, M., Comportement des robots parallèles à mouvements découplés et corps déformables, Congrès Français de Mécanique, (2005).
11. Raţ, N.R., Neagoe, M., Stan, S.D. ,Comparative Dynamic Analysis of Two Parallel Robots, The 2010 International Conference on Robotics (ROBOTICS'10), Vols. 166-167 ,pp 345-356, (2010).
12. Ibrahim, O., Contribution a la modelisation dynamique des robots parallels et des robots hybrids, PHD thesis, L'Ecole Centrale de Nantes et l'Universite de Nantes, (2006).
13. Gogu, G., Structural synthesis of fully-isotropic translational parallel robots via theory of linear transformations, European Journal of Mechanics A/Solids 23, pp. 1021–1039, (2004).
14. Gogu, G., *Structural synthesis of parallel robots*, Part 1: Methodology, Springer Verlag, (2008).

15. Gogu, G., *Structural synthesis of parallel robots*, Part 3: Topologies with planar motion of the moving platform, Springer Verlag, (2010).
16. Gogu, G., Optimization on the modeling of industrial robots (in Romanian), PHD thesis, Transilvania University of Brasov, (1995).
17. Costa, A., Jones, R.P., Automitive Vehicle Chassis Simulation for Motion Control Studies using Multibody Systems (MBS) Modelling Techniques, SAE Paper No. 921443, (1992).